International Journal of Innovative Computing, Information and Control
Volume **20**, Number **3**, June **2024**

ICIC International ©2024 ISSN 1349-4198
pp. 965–978

HIGH-PRECISION MODELLING-BASED POWER BATTERY STATE ESTIMATION AND ACTIVE BALANCING

Xin Ye[1], Yongwen Song[1,*], Csaba Csiszár[2], Bálint Csonka[2] and Dávid Földes[2]

[1]School of Vehicle Engineering
Chongqing University of Technology
No. 69, Hongguang Avenue, Banan District, Chongqing 400054, P. R. China
yexin@cqut.edu.cn; *Corresponding author: songyongwenki@163.com

[2]Department of Transport Technology and Economics
Faculty of Transportation Engineering and Vehicle Engineering
Budapest University of Technology and Economics
Műgyetem rakpart 3, Budapest 1111, Hungary
{ csiszar.csaba; csonka.balint; foldes.david }@kjk.bme.hu

Received August 2023; revised December 2023

Abstract. *Power battery state estimation is the cornerstone of BMS (Battery Management System), and active balancing technology is the core function of BMS. The accuracy of state estimation is limited by the accuracy of the model. To improve the accuracy of state estimation, the solid-state diffusion in the electrochemical mechanism is considered to update the open-circuit voltage, and a high-precision battery model is obtained. Next, the applicability of three estimation algorithms is compared, and joint estimation of SOC (State of Charge) and SOH (State of Health) is achieved based on the high-precision model and dual-capacity Kalman filtering, and the effect of model improvement and algorithm optimization is simulated and verified under multiple dynamic working conditions. Finally, a "peak shaving and valley filling" parallel balancing strategy is formulated using battery SOC as the variable, and simulation is conducted on a bidirectional flyback converter balancing system for four single cells under different degrees of imbalance with a discreteness value of 10%. The results show that battery state estimation based on a high-precision model can effectively reduce estimation errors throughout the full SOC range and improve inconsistency among the cells in the battery pack with the active balancing technology.*

Keywords: Power battery, BMS, Electrochemical mechanism, Dual-capacity Kalman filter, Bidirectional flyback converter

1. **Introduction.** With the increasing global attention and concern for environmental issues in recent years, the development of electric vehicles has reached a climax. However, the efficiency and safety of the power battery, as the core power source, have attracted market attention. Therefore, more and more scholars are involved in the research of battery management system. The battery state estimation, as the core and foundation of the system, and the battery pack balancing technology that relates to safety and efficiency become the main topics of this research.

With the rise of new energy vehicles, the battery management system has always played an important role. In the long process of updating and iterating the battery management system, the battery SOC estimation and balancing technology have been gradually optimized and improved, making BMS better able to meet production and market demand.

DOI: 10.24507/ijicic.20.03.965

In the early stage, the commonly used methods for battery SOC estimation were ampere-hour integration or open circuit voltage method, but they were gradually replaced by new methods due to their poor accuracy and implementation difficulties. In 2015, Fan et al. [1] combined these two traditional methods and solved the problem of inaccurate initial value of ampere-hour integration. Although this method has improved the accuracy, it requires higher accuracy of open circuit voltage measurement. In 2016, Shi et al. [2] estimated battery SOC with extended Kalman filter based on Thevenin battery model. In 2018, Gao et al. [3] compared EKF and UKF and proposed the unscented Kalman filter algorithm with better convergence and higher accuracy for estimating battery SOC. In the same year, Xie et al. [4] used the unscented particle filter theory to estimate battery SOC, but the particle filter is sensitive to disturbances and has poor robustness. Furthermore, in 2019, Wang et al. [5] used the SSRCKF algorithm to estimate battery SOC, further improving the robustness of the system. The above adaptive SOC estimation methods based on battery models have shown more accurate results with the optimization of algorithms [6], but they greatly rely on the accuracy of the battery model. In recent years, the application of big data models has developed in various forms. In 2021, Cao et al. [7] implemented the battery SOC estimation under multiple complex operating conditions based on the NARX neural network improved by the enhanced cuckoo search algorithm. In 2023, Hu et al. [8] proposed the battery SOC estimation combining gated recurrent unit neural network with EKF. From the research results, neural network models have played a huge advantage in battery SOC estimation. However, due to the high computational and maintenance costs of this method, it has not been used in the actual application of power battery state estimation. In summary, considering accuracy, robustness and applicability, model-based adaptive algorithms are better suited to solve the problems of the current battery management system. To further improve this method, we focus on the influence of battery aging and model accuracy, and propose a high-precision battery model based on the improved equivalent circuit model of electrochemical mechanism, and combine double-capacity Kalman filtering to achieve battery SOC-SOH estimation and real-time updates of usable battery capacity. In addition, the battery pack balancing management technology is also constantly developing. In the 1990s, the resistance shunt method was used to achieve balancing management, including Lindemark in 1991 [9] and Kutkut and Divan in 1996 [10]. However, by 2013 and 2015, Xu et al. [11], and Tang [12] realized balancing through the design of a switch resistance balancing topology. This method reduces balancing loss, but still belongs to passive balancing. To improve the efficiency of battery pack balancing, in 2016, Feng et al. [13] proposed a capacitance active balancing circuit that regulates controllable switches to transfer energy between batteries. Considering the limitations of capacitance balancing, in 2018, Wang [14] and Zhu [15] studied transformer balancing topology, which has a large current and high efficiency, but also has a large spatial volume. In 2019, Qays et al. [16] designed an Any-Cells-to-Any-Cells balancing topology based on the Buck-Boost circuit, which has a small spatial volume but slow balancing speed. Therefore, in 2021, Zhu et al. [17] once again designed an active balancing system based on bidirectional flyback transformer balancing to further reduce the loss of unidirectional transformer balancing and avoid electromagnetic interference. Although it still has the disadvantage of slightly larger volume, considering balancing efficiency and reliability, this balancing structure is deemed more suitable for efficient balancing in battery management systems. In recent years, solutions that integrate active and passive balancing have also been proposed, such as Liu et al. [18] in 2022, who proposed an adaptive selection strategy for active and passive balancing, and Liao et al. [19] in 2023, who proposed a time optimization algorithm for active and passive balancing. However,

these solutions have shortcomings such as poor reliability, high cost, and lack of compactness. After evaluation, bidirectional flyback converter is more suitable for the balancing requirements of power battery packs, so this research is based on this solution.

Based on this, we will use a high-precision model and double-capacity Kalman filtering to jointly estimate SOC-SOH, and use bidirectional flyback converter to implement active balancing management for battery packs. The first part of this paper analyzes the current research status and analysis of battery SOC estimation and balancing technology. The second part establishes a high-precision battery model. The third part conducts electrical characteristic experiments and model parameter identification. The fourth part uses the high-precision model and double-capacity Kalman filtering for state estimation. The fifth part researches on active balancing management based on bidirectional flyback converter. Finally, the last part is the conclusion and outlook of our research.

2. **Establishment of High-Precision Battery Model.** Combining practical application scenarios and target requirements, the electrochemical mechanism model can characterize the internal electrochemical reaction characteristics and is considered a high-precision battery model. Currently, the most accepted model is the quasi-two-dimensional model based on the porous electrode structure (P2D model). However, this model is computationally complex and is not suitable for electric vehicles. Figure 1 shows the working process of the power battery explained by the P2D principle, where x represents the direction of lithium-ion liquid-phase diffusion in the macroscopic dimension, and r represents the direction of lithium-ion solid-phase diffusion inside the electrode in the microscopic dimension. Macroscopically, there is charge transfer and double layer formation at the electrode solid-liquid interface, SEI film and membrane voltage drop of lithium ion, and concentration polarization caused by the difference in lithium-ion transfer speed between internal and external regions. Microscopically, lithium ions diffuse from the center of the electrode to the surface. However, according to the equivalent circuit model, the output electromotive force of the power battery can be expressed as Equation (1), where U_L is the terminal voltage, U_{OCV} is the open circuit voltage, and SOC_{avg} is the average SOC of the battery. U_{ohm} is the ohmic polarization voltage, U_{dl} is the double-layer polarization

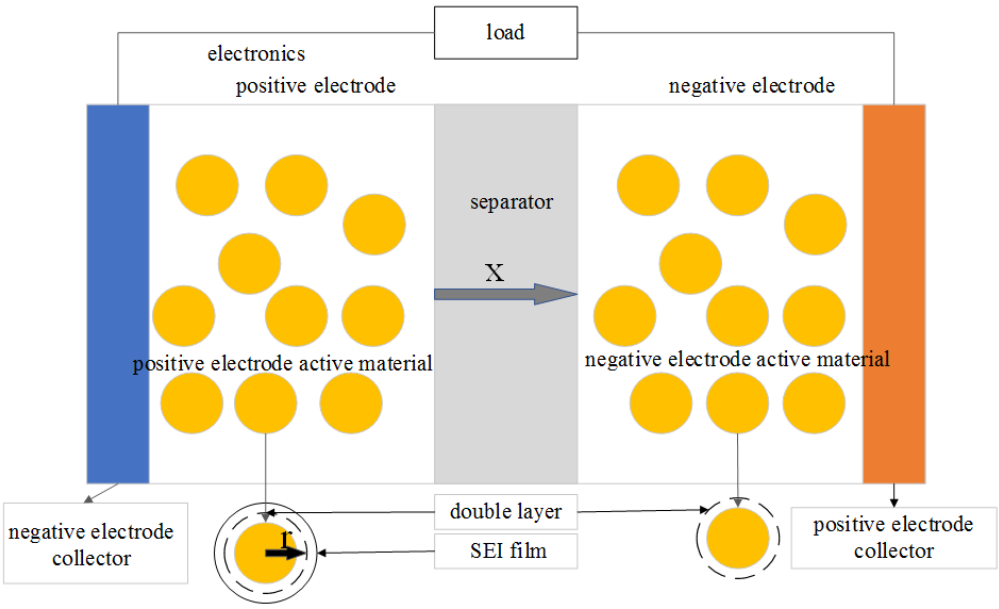

FIGURE 1. Schematic diagram of battery structure and working process

voltage, and U_{conc} is the concentration polarization voltage. The polarization reaction at the electrode has a cumulative effect on the terminal voltage, and the SEI film has a high response frequency. The second-order RC model can characterize the electrochemical reaction of the battery at the macro level. Therefore, the equivalent circuit model is commonly used as an engineering battery model.

$$U_L = U_{OCV}\left(SOC_{avg}\right) - U_{ohm} - U_{dl} - U_{conc} \tag{1}$$

Based on this, the present study considers the reaction mechanism at the microscopic level and establishes a high-precision battery model. According to the solid-phase diffusion mechanism, the actual lithium ion concentration participating in the electrochemical reaction is the surface concentration of the electrode, not the average concentration. Equation (2) represents the macro manifestation of the surface lithium ion concentration, i.e., the surface SOC, where $C_{i,surf}$ represents the surface lithium ion concentration involved in the reaction during electrode operation, and $C_{i,\max}$ represents the internal lithium ion concentration of the electrode when the battery is fully charged. $i = n$ or s represents the positive and negative electrodes, respectively.

$$SOC_{surf} = \frac{C_{i,surf} - C_{i,lower}}{C_{i,\max}} \tag{2}$$

The surface SOC of the battery can be calculated using Equation (3), where ΔSOC is the macroscopic manifestation of diffusing lithium ion concentration, and its electrochemical model formula is a complex partial differential equation. Therefore, it can be simplified using a linear approximation of a four-parameter sixth-order polynomial, as shown in Equation (4).

$$SOC_{surf} = SOC_{avg} - \Delta SOC \tag{3}$$

$$\Delta SOC = R_{sd1} I_f (1 - \exp(-t/\tau_{sd1})) + R_{sd2} I_f (1 - \exp(-t/\tau_{sd2})) \tag{4}$$

In this equation, $R_{sd1,2}$ and $\tau_{sd1,2}$ represent the fitting coefficients of linear approximation for solid-state diffusion, while I_f represents Faraday current related to double-layer polarization, which can be determined by $I_f = U_{dl}/R_{CT}$. With the improvement of the solid-state diffusion mechanism, the output electromotive force of the battery can be represented by Equation (5).

$$U_L = U_{OCV}(SOC_{surf}) - U_{ohm} - U_{dl} - U_{conc} \tag{5}$$

At this point, the open-circuit voltage is obtained by looking up the SOC_{surf} table, while the double-layer polarization voltage and concentration polarization voltage are calculated through a second-order RC model. Therefore, this study incorporates liquid-phase diffusion polarization based on the work of Liu et al. [20] and establishes an Electrochemistry-based Equivalent Circuit Model (EECM), as shown in Figure 2, which includes important parameters to be identified, as listed in Table 1, where I represents the current source, $U_{OCV}(SOC_{surf})$ represents the open circuit voltage based on SOC_{surf}, and ΔSOC_1 and ΔSOC_2 represent the two components of SOC change during solid-phase diffusion process.

3. **Experimental and Parameter Identification.** According to statistics, the global number of electric vehicles equipped with ternary lithium batteries far exceeds 33 million units. Meanwhile, taking account of the maximum charge and discharge current of the charger, this study selected ternary lithium batteries with a capacity of 3.4 Ah and a nominal voltage of 3.7 V as the experimental object. The equipment used was a Neware battery testing system with an accuracy of within ± 0.01 A, and the highest data acquisition frequency was no more than 10 Hz. The parameters of the lithium-ion battery to be tested are shown in Table 2.

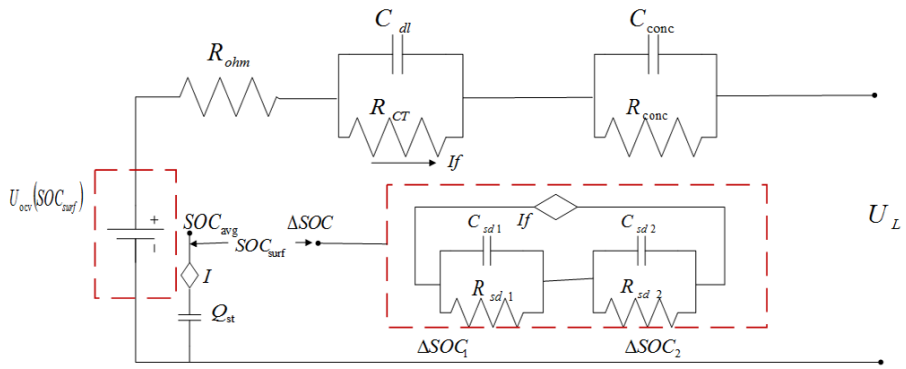

FIGURE 2. The structure of EECM

TABLE 1. Unidentified parameters of the EECM model

Unidentified	Parameter description
R_{CT}	The Charge Transfer Resistance (CTR)
C_{dl}	Double Layer Capacitance (DLC)
R_{conc}	Concentration Polarization Resistance (CPR)
C_{conc}	Concentration Polarization Capacitance (CPC)
$R_{sd,1,2}$	The transient resistance of solid-phase diffusion
$C_{sd,1,2}$	The transient capacitance of solid-phase diffusion
R_{ch}/R_{dis}	Discharge/charge ohmic internal resistance

TABLE 2. The performance parameters of the single cell to be tested

Project	Parameters
Battery category	NCR18650B
Rated capacity (Ah)	3.4
Nominal voltage (V)	3.7
Cutoff voltage (V)	charging: 4.2, discharging: 2.75
Maximum charging/discharging current (A)	10/4
DC internal resistance (mΩ)	15-30

The experimental equipment cannot accurately obtain an open-circuit voltage curve using the microcurrent discharge method. Therefore, a constant-current pulse charging and discharging method was used to obtain the SOC-OCV curve of the battery. Twenty-one SOC values were recorded and averaged to obtain the actual open-circuit voltage value. After precision comparison, a ninth-order polynomial fitting (as shown in Equation (6)) was used to obtain the curve shown in Figure 3. In addition, the experimental HPPC and DST condition data of the battery were obtained, which can be used as a basis for identifying model parameters and as a reference for accuracy validation.

$$f(x) = 552x^9 - 2354x^8 + 4229x^7 - 4177x^6 + 2495x^5 - 994x^4 + 234.7x^3 - 39.9x^2 + 5.541x + 3.012 \quad (6)$$

After comparing various parameter identification methods, considering the large number of model parameters after improvement, this study used a particle swarm optimization algorithm for global optimization, with a given fitness function and value range. It should be emphasized that the open-circuit voltage value at this point is obtained by looking up the SOC-OCV curve using SOC_{surf}, not SOC_{avg}.

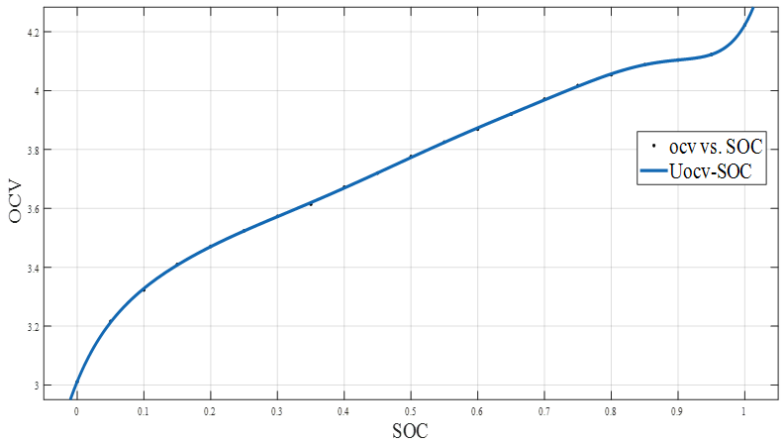

FIGURE 3. SOC-OCV fitting curve

In order to verify the universality and accuracy of the battery model, this section further validated the identified model using the Dynamic Stress Test (DST) condition.

Figures 4 and 5 respectively show the simulation results of the SOC range between 40% and 50% and between 0 and 10% from the entire DST condition. Figures 6 and 7 illustrate the errors in these two ranges. From the simulation results, it is evident that the ECM model error is far greater than the EECM model error in the SOC range of 0

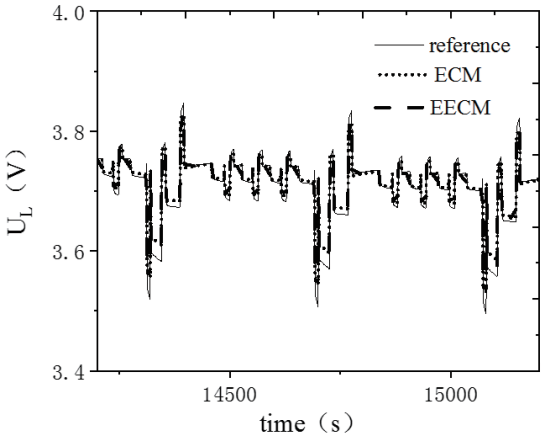

FIGURE 4. Comparison of model voltage (SOC = 40%∼50%)

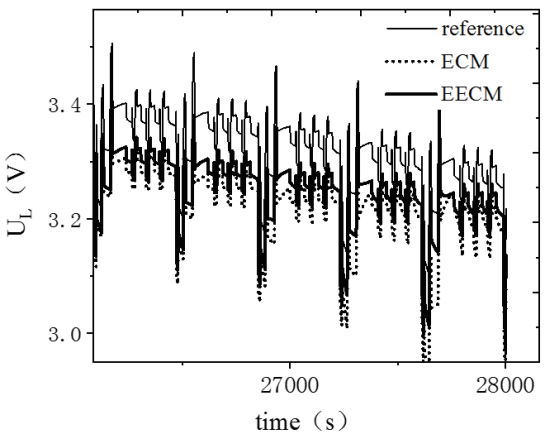

FIGURE 5. Comparison of model voltage (SOC = 0∼10%)

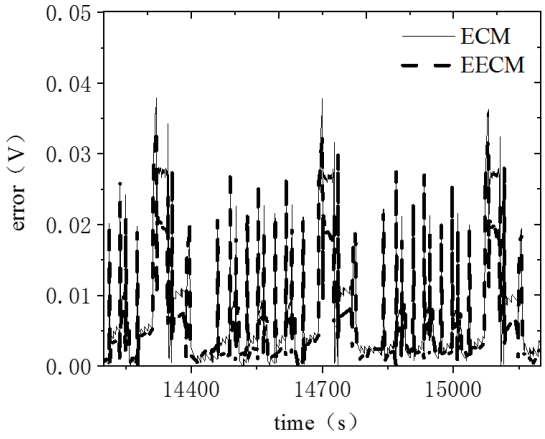

FIGURE 6. Error of model voltage (SOC = 40%∼50%)

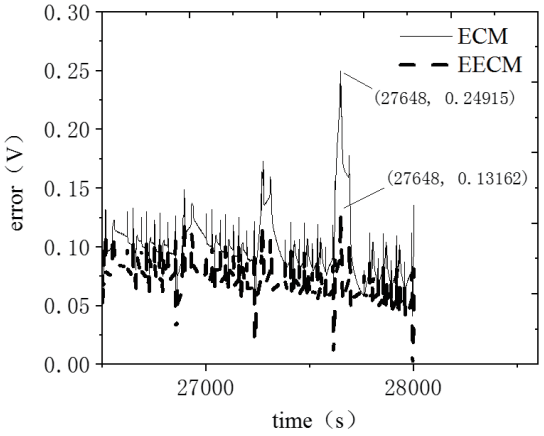

FIGURE 7. Error of model voltage (SOC = 0∼10%)

to 10%, whereas the simulation accuracy of both models is similar for the range between 40% and 50%. The main reason for this phenomenon is that polarization intensifies in the later stage of discharge, and the ECM model does not consider the effect of solid-state diffusion polarization on the model accuracy.

Based on the above comparative analysis, it is concluded that the accuracy of the EECM model is superior to that of the ECM model, especially in compensating for the large error of the ECM model at the end of battery discharge. At the same time, considering the usage characteristics and cost of power batteries, even if the electrochemical mechanism model and neural network model show better accuracy advantages, they are still not suitable for the development of practical power battery management system models due to their high computational difficulty and cost. Therefore, these models are not adopted in this study.

4. **Battery State Estimation Based on High-Precision Model.** As the battery is a nonlinear time-varying system, estimation algorithms derived from the Kalman filter include three kinds of nonlinear Kalman filter algorithms: Extended Kalman Filter (EKF), Unscented Kalman Filter (UKF), and Cubature Kalman Filter (CKF). Compared with EKF, UKF and CKF are both sampling-based filtering algorithms. However, the UT transformation used in UKF does not have strong mathematical theoretical support, while the CKF takes the third-order radial spherical volume criterion as the sampling basis. At the same time, the reliability of the integration formula is usually evaluated by a reliability

factor I. As the dimension of the state variable increases, the reliability of UKF becomes worse, while the reliability of CKF remains at 1. CKF is an excellent filtering algorithm in terms of applicability, reliability, accuracy, and execution efficiency, especially compared to UKF in handling high-dimensional systems. The state equation and output observation equation of the pseudo system can be represented by Equation (7):

$$\begin{cases} x_{k+1} = f(x_k, u_k) + \omega_k \\ y_{k+1} = h(x_k, u_k) + \nu_k \end{cases} \tag{7}$$

ω_k and ν_k are respectively process noise and observation noise, both mutually independent Gaussian white noise. For CKF, the basic idea is to use the third-order radial spherical volume rule to integrate the n-dimensional integration formula, constructing $2n$ volume points as shown in Equation (8), where, $\xi_i = \sqrt{n}[1]i$, $\omega_i = 1/2n$, $i = 1, \ldots, 2n$ and $[1]i = [1 * In, -1 * In]$, $In \subset Rn$ is the unit matrix.

$$In(f) = \int_{Rn} f(x)N(x; 0, I)dx \approx \sum_{i=1}^{2n} \omega_i f(\xi_i) \tag{8}$$

To apply CKF in battery SOC estimation, firstly, the initialization of initial state value and covariance P_0 is done by referring to SOC-OCV curve table. Then, process noise Q and observation noise R are set and used in the Cubature Kalman Filter algorithm for estimation. Therefore, based on the EECM model, the state variables for estimation are $x_{k+1} = (SOC_{surf,k+1}; U_{dl,k+1}; U_{conc,k+1}; \Delta SOC_{1,k+1}; \Delta SOC_{2,k+1})$, and the SOC to be estimated can be obtained by $SOC_{k+1} = SOC_{surf,k+1} + \Delta SOC_{1,k+1} + \Delta SOC_{2,k+1}$. $\omega_{i,k}$, $i = 1, 2, 3, 4, 5$ are the noise during the simulation process, and ν_{k+1} represents the noise during observation. Considering the effect of internal resistance on battery SOC estimation, a DCKF filter is established to estimate the Ohmic internal resistance in real time, in order to enhance the accuracy of battery SOC estimation.

To demonstrate the comparison of the EECM model and the ECM model under DST conditions, the SOC estimation effect diagram in the low SOC stage is extracted and shown in Figure 8. It can be seen from the figure that in the low SOC stage, the advantage of the EECM model is more obvious. Meanwhile, Figure 9 shows the impact of real-time estimated internal resistance on battery SOC. It can be seen from the figure that the real-time updated Ohmic internal resistance makes the estimation model exhibit better convergence and higher accuracy, with a higher fault-tolerant rate, ensuring the normal and reliable operation of electric vehicles.

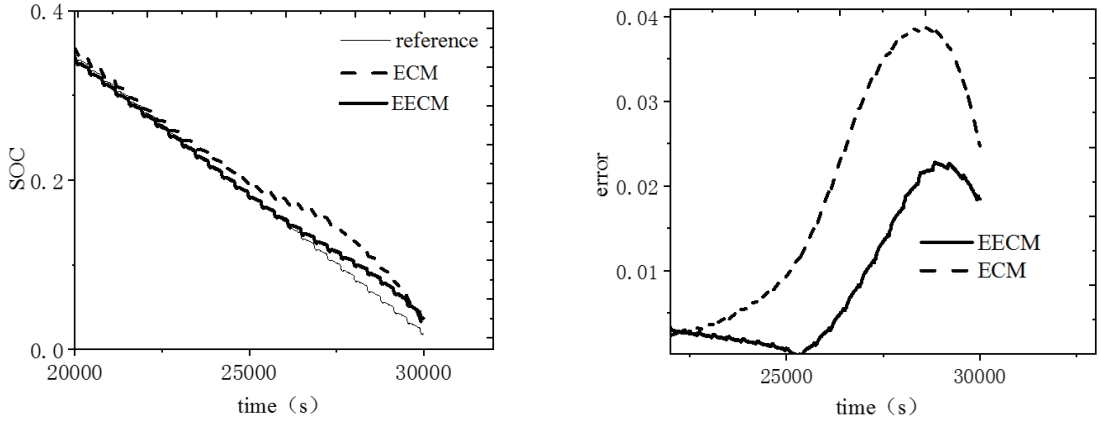

FIGURE 8. Comparison of the estimation effect based on EECM

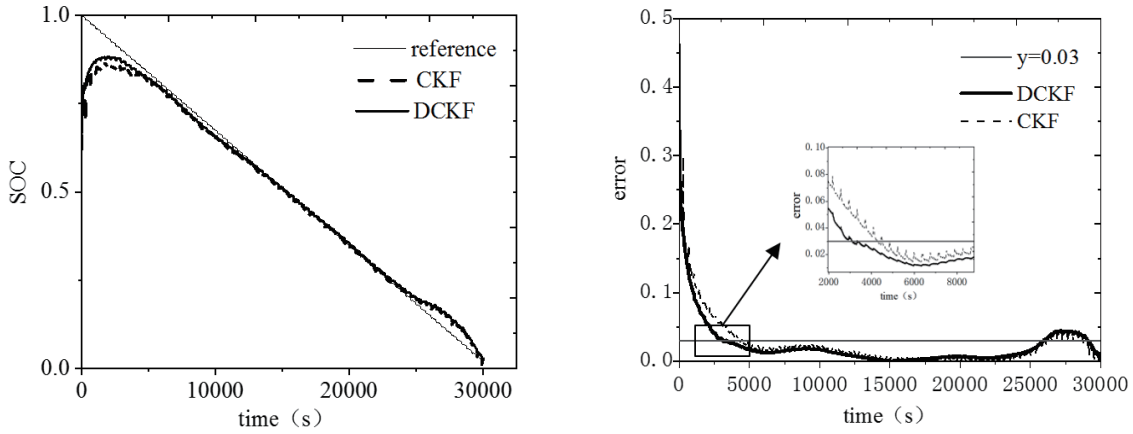

FIGURE 9. Comparison of the estimation effect based on DCKF

5. **Bidirectional DC-DC Converter Active Balancing Control.** The topology structure of the bidirectional flyback converter balancing system is shown in Figure 10 and can be divided into two parts: the yellow part is connected to the primary side of the transformer, which absorbs energy, while the blue part is connected to the secondary side of the transformer, which consumes energy. Taking a four-cell battery as an example, we simulate the designed balancing system. The bidirectional flyback converter can achieve bidirectional energy transfer from a single cell to another cell and avoid repeated charge and discharge of the battery, reducing energy loss. Compared with the basic flyback type balancing topology, it further improves efficiency. The entire circuit structure uses a PWM signal to control two MOSFET transistors based on the single-ended flyback converter circuit, and the transformer is used as the symmetry axis to achieve left-right symmetry. Its operating process is similar to that of the flyback converter.

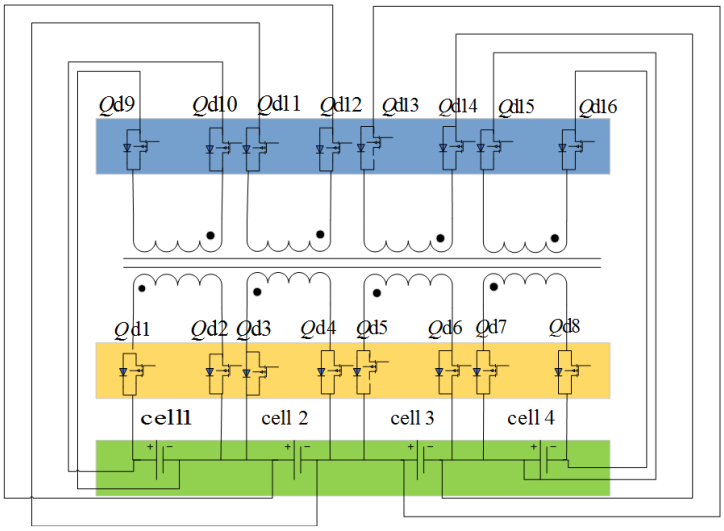

FIGURE 10. (color online) Topology of bidirectional flyback converter balancing

The balance control system requires a threshold to determine when to turn on and off the balance. Therefore, the more accurate SOC estimated earlier is selected as the balance variable. The range value $\delta = SOC_{\max} - SOC_{\min}$ in the battery pack can reflect the maximum dispersion of the overall electricity, so in this study, δ is used as the criterion for judging the battery inconsistency. Considering the changes in battery performance

parameters, the starting threshold for balance is set as $\delta \geq 0.2\%$, and the closing threshold for balance is set as $\delta \leq 0.1\%$. Meanwhile, considering the complex and variable imbalance conditions, such as the ones shown in Table 3, this study adopts a "peak shaving and valley filling" parallel balance strategy, as shown in Figure 11.

TABLE 3. Description of the imbalance conditions

Imbalance condition	Concrete description
Single high, multiple low	$Cell_{\max} > Cell_{avg} > Cell_1 > Cell_2 > Cell_{\min}$
Multiple high, multiple low	$Cell_{\max} > Cell_1 > Cell_{avg} > Cell_2 > Cell_{\min}$
Multiple high, single low	$Cell_{\max} > Cell_1 > Cell_2 > Cell_{avg} > Cell_{\min}$

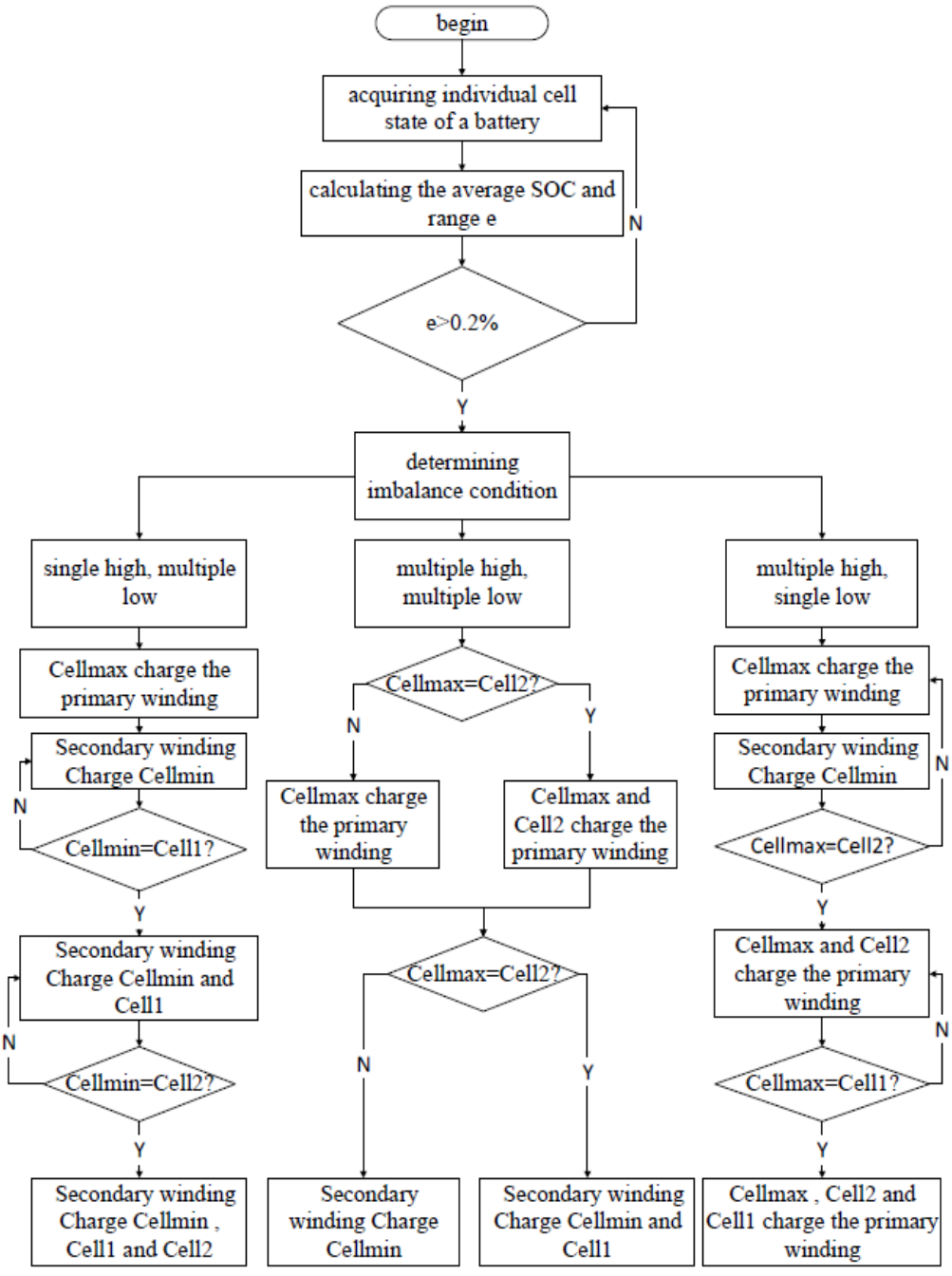

FIGURE 11. Battery "peak shaving and valley filling" parallel balancing strategy

A simulation model was built in the MATLAB/Simulink environment to compare and verify the "peak shaving and valley filling" parallel bidirectional flyback converter balance under three operating modes. Four single battery cells were set from the initial 90% SOC to 80% SOC, and the three types of imbalances mentioned above were simulated. The simulated system parameters are shown in Table 4.

Table 4. Simulation parameter settings for balancing system

Parameter	Numerical value
Switching frequency	10 KHz
Turns ratio	1 : 1 : 1 : 1
Primary-secondary coupling inductance	20 μH
Duty cycle	50%

The comparison of the balancing effects between the bidirectional flyback converter and the basic flyback converter under three operating modes is shown in Figure 12. The balancing current for both is set at 3.5 Ah. Observing the balancing effect of the bidirectional flyback converter vertically, regardless of the mode, the system can quickly complete the balancing within 1200 s for an SOC difference of 10%, compared to the balancing system of the basic flyback converter. As shown in Figures 12(a), 12(c), and 12(e) represent the balancing effect of the bidirectional flyback converter balancing structure under three modes, while Figures 12(b), 12(d), and 12(f) represent the balancing effect of the single-ended flyback converter under the same three conditions. It can be seen from the figure that the balancing time is shortened by 80%, 70%, and 60%, respectively, under the three different modes. This is because the originally independent "peak shaving" and "valley filling" operating modes can cause the battery to repeat ineffective energy transfer.

6. **Conclusion.** By considering the solid-state diffusion polarization in the electrochemical mechanism, the EECM model is improved to enhance the accuracy of the model over the entire SOC range, especially in the low SOC range. Then, the CKF is used to establish a DCKF filter to estimate the battery's SOC and real-time update the ohmic internal resistance to improve accuracy. Finally, using four single battery cells as an example, a "peak shaving and valley filling" parallel balancing system based on bidirectional flyback conversion is proposed, and the balance effect is simulated and compared in MATLAB/Simulink, validating its higher balance efficiency. However, the influence of temperature, an important factor affecting the model's accuracy, is ignored, which results in poor applicability. Secondly, the research object of the balancing system is small, and the set environment and conditions are relatively ideal. In practical applications, the influence of factors such as series-parallel connection method and internal temperature rise needs to be considered. Therefore, in the next research work, it is possible to further consider the influence of temperature and aging on battery models and state estimation, and analyze the balancing requirements within and between battery packs to provide practical and feasible battery state estimation and balancing management solutions for battery management systems.

Acknowledgment. This work was supported by the National Natural Science Foundation of China under Grant 62241201, Chongqing Natural Science Foundation general project under Grant CSTB2023NSCQ-MSX0418, and the Ministry of Innovation and Technology of Hungary from the National Research, Development and Innovation Fund under Project no 2019-2.1.11-TÉT-2020-00176.

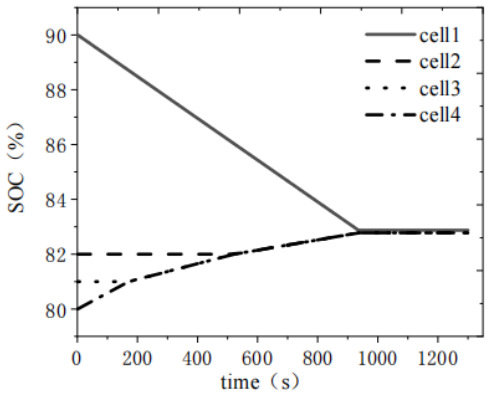

(a) Balancing effect of Uni-High Multi-Low bidirectional flyback converter

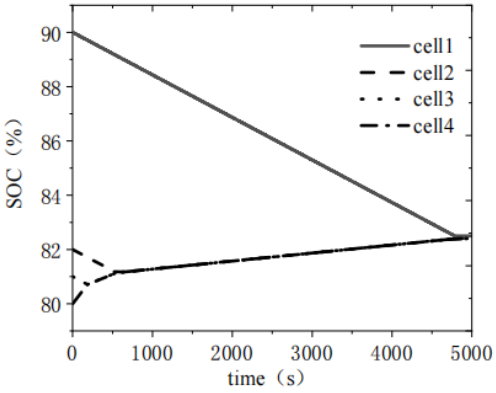

(b) Balancing effect of the Uni-High Multi-Low single-ended flyback converter

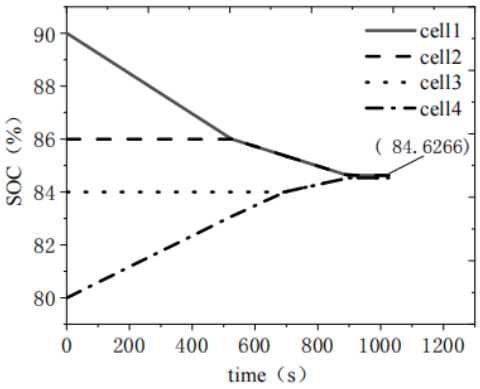

(c) Balancing effect of Multi-High Multi-Low bidirectional flyback converter

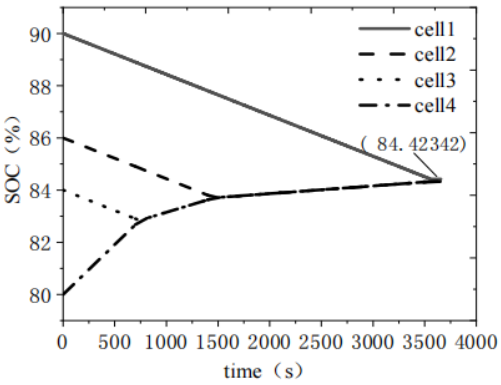

(d) Balancing effect of Multi-High Multi-Low single-ended flybac flyback converter

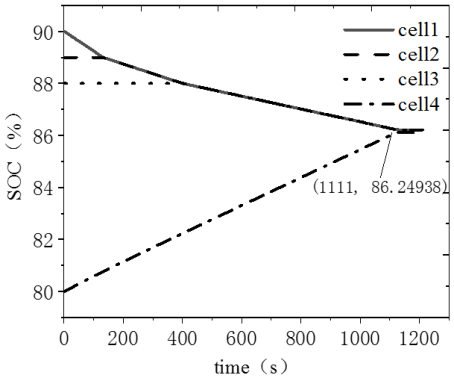

(e) Balancing effect of Multi-High Uni-Low bidirectional flyback converter

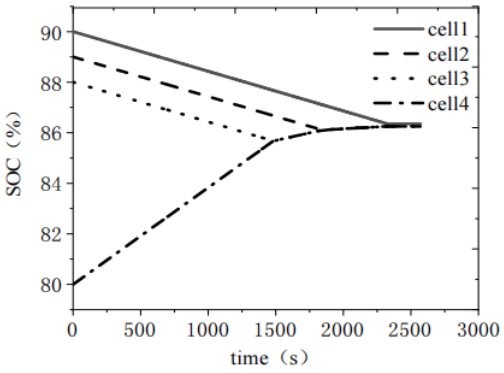

(f) Balancing effect of Multi-High Uni-Low single-ended flybac flyback converter

FIGURE 12. Comparison of balancing effects under three modes

REFERENCES

[1] X. Fan, Q. Zeng and X. Zhang, SOC estimation and simulation study of electric vehicle battery based on improved ampere-hour integration method, *Electrical Application*, vol.34, no.8, pp.111-115, 2015.

[2] H. Shi, W. Yang, Q. Feng et al., Accurate estimation of state of charge for electric vehicle batteries based on EKF filtering algorithm, *Power Supply Technologies*, vol.40, no.2, pp.361-364, 2016.

[3] J. Gao, T. Ai, X. Xu et al., Charge state estimation strategy of LiFePO4 battery based on UKF, *Electronic Measurement Technology*, vol.41, no.3, pp.12-16, 2018.

[4] C. Xie, Y. Fei, C. Zeng et al., State estimation of vehicle lithium-ion battery based on unscented particle filter, *Transactions of China Electrotechnical Society*, vol.33, no.17, pp.3958-3964, 2018.
[5] H. Wang, S. Wang and Y. Zhang, Estimation of SOC for lithium-ion battery based on SSRCKF algorithm, *Battery*, vol.49, no.4, pp.301-304, 2019.
[6] Q. Liu, D. Xu, B. Jiang and Y. Ren, Prescribed-performance-based adaptive control for hybrid energy storage systems of battery and supercapacitor in electric vehicles, *International Journal of Innovative Computing, Information and Control*, vol.16, no.2, pp.571-583, 2020.
[7] X. Cao, F. Peng, L. Li et al., State of charge estimation of lithium-ion battery based on IBAS-NARX neural network, *Energy Storage Science and Technology*, vol.10, no.6, pp.2342-2351, 2021.
[8] M. Hu, G. Zhu, C. Liu et al., Joint estimation of SOC for lithium-ion battery based on Kalman filter with hysteresis and gated recurrent unit neural network, *Automotive Engineering*, vol.45, no.9, pp.1688-1701, 2023.
[9] B. Lindemark, Individual cell voltage equalizers (ICE) for reliable battery performance, *International Telecommunications Energy Conference (INTELEC)*, pp.196-201, 1991.
[10] N. H. Kutkut and D. M. Divan, Dynamic equalization techniques for series battery stacks, *International Telecommunications Energy Conference (INTELEC)*, pp.514-521, 1996.
[11] C. Xu, G. Yan, J. Li and Y. Quan, Design of lithium-ion battery management system with balancing control function, *Power Supply Technologies*, vol.37, no.6, pp.959-962, 2013.
[12] T. Tang, *Design of Lithium-ion Battery Pack Management System*, Ph.D. Thesis, Anhui University, 2015.
[13] N. Feng, L. Chen and J. Tang, Research on capacitive balancing system for series battery pack, *Journal of Chongqing University of Technology (Natural Science Edition)*, vol.30, no.1, pp.1-6, 2016.
[14] J. Wang, *Research and Implementation of Active Balancing Control Strategy for Electric Vehicle Battery Pack*, Master Thesis, Jilin University, 2018.
[15] X. Zhu, *Research on Active Balancing Technology for Power Battery Pack with Transformer Isolation*, Master Thesis, Zhejiang University, 2018.
[16] M. O. Qays, Y. Buswig and M. Anyi, Active cell balancing control method for series-connected lithium-ion battery, *International Journal of Innovative Technology and Exploring Engineering*, vol.8, pp.2424-2430, 2019.
[17] E. Zhu, Y. Li, S. Chen et al., Design of lithium-ion battery pack balancing system based on bidirectional flyback converter, *Sensors and Microsystems*, vol.40, no.3, pp.77-80, 2021.
[18] W. Liu, Y. Wang, Y. Xu et al., Energy balancing method for on-board lithium-ion battery power based on adaptive selection of active and passive balancing topology, *Chinese Journal of Scientific Instrument*, vol.43, no.2, pp.244-252, 2022.
[19] L. Liao, J. Zhang, Y. Wang et al., Active and passive balancing of lithium-ion battery based on time optimization algorithm, *Battery*, vol.53, no.4, pp.393-397, 2023.
[20] M. Ouyang, G. Liu, L. Lu et al., Enhancing the estimation accuracy in low state-of-charge area: A novel onboard battery model through surface state of charge determination, *Journal of Power Sources*, vol.270, no.1, pp.221-237, 2014.

Author Biography

Xin Ye (IEEE Member) received the B.S. degree in Mechanical Engineering from Chongqing University, China in 2004; and the Ph.D. degree in Vehicle Engineering from Chongqing University, China in 2011. She is currently an associate professor with the School of Vehicle Engineering, Chongqing University of Technology, Chongqing, China.

Her research fields include new energy and intelligent vehicle integrated control, intelligent algorithm research and so on.

Yongwen Song received her bachelor's degree in Automotive Service Engineering from the School of Energy and Power Engineering at North University of China in Taiyuan in 2020. She obtained her master's degree in Vehicle Engineering at Chongqing University of Technology in 2023. At present, she is working in Shenzhen Growatt New Energy Co., Ltd., engaged in the development of battery algorithms.

Her research mainly focused on battery management for new energy electric vehicles, including battery electrochemical models, battery state estimation, and battery active equalization management, during her master's program.

Csaba Csiszár received his Ph.D. degree in Transportation Science in 2002, fulfilled the habilitation requirements in 2020, and obtained the D.Sc. degree in 2022. He works as a full professor at Department of Transport Technology and Economics, Budapest University of Technology and Economics. His research area covers topics in transport informatics and passenger transportation systems, with a special focus on system integration, electromobility, and mobility based on autonomous vehicles. He is the author of over 200 scientific papers, the number of independent citations is over 1000, and his H-index is 20. He gave guest lectures at several foreign universities. 7 Ph.D. students defended the Ph.D. degree under his supervision. He is an elected member of the Committee of Transport and Vehicle Sciences at the Hungarian Academy of Sciences.

Bálint Csonka received his Ph.D. degree in Transportation Technology Science on the topic of the Development of Electromobility Services from the Budapest University of Technology and Economics in 2020. He is currently a research associate with the Budapest University of Technology and Economics. His research area is the development of methods to support the operation of electric vehicles and charging infrastructure, and the optimization of local energy production and storage capacities. He has published and peer-reviewed more than 100 articles in high-ranked journals.

Dávid Földes received his Ph.D. degree in Transportation Science in 2019; the title of his dissertation is 'Development of Innovative Transport Systems and Mobility Services'. He won the European Friedrich-List Award 2020 in the category Ph.D. dissertation. He works at the Department of Transport Technology and Economics, at Budapest University of Technology and Economics as a research associate. Since 2021, he has been a Ph.D. supervisor for students in Transportation Science. His research areas cover micromobility, shared mobility, electromobility, and autonomous vehicle-based mobility services with special regard to travellers' habits and expectations. He has more than 60 scientific publications, his number of independent citations is more than 315, and his H-index is 12.